Trans Membrane Domain IV Is Involved in Ion Transport Activity and pH Regulation of the NhaA-Na^+/H^+ Antiporter of *Escherichia coli*†

Livnat Galili, Andrea Rothman, Lena Kozachkov, Abraham Rimon, and Etana Padan*

Alexander Silberman Institute of Life Sciences, Hebrew University of Jerusalem, 91904 Jerusalem, Israel

Received August 13, 2001; Revised Manuscript Received November 6, 2001

ABSTRACT: We have previously shown that the activity of NhaA is regulated by pH and found mutations that affect dramatically the pH dependence of the rate but not the K_m (for Na^+ and Li^+) of NhaA. In the present work, we found that helix IV is involved both in ion translocation as well as in pH regulation of NhaA. Two novel types of NhaA mutants were found clustered in trans membrane segment (TMS) IV: One type (D133C, T132C, and P129L) affects the apparent K_m of NhaA to the cations with no significant effect on the pH profile of the antiporter; no shift of the pH profile was found when the activity of these mutants was measured at saturating Na^+ concentration. In contrast, the other type of mutations (A127V and A127T) was found to affect both the K_m and the pH dependence of the rate of NhaA whether tested at saturating Na^+ concentration or not. These results imply that residues involved in the ion translocation of NhaA may (A127) or may not (D133, T132, and P129) overlap with those affecting the pH response of the antiporter. All mutants cluster in the N-terminal half of the putative α-helix IV, one type on one face, the other on the opposite. Cys accessibility test demonstrated that although D133C is located in the middle of TMS IV, it is inhibited by *N*-ethylmaleimide and is exposed to the cytoplasm.

Sodium proton antiporters are ubiquitous membrane proteins found in the cytoplasmic and organelle membranes of cells of many different origins, including plants, animals, and microorganisms. They are involved in cell energetics, and play primary roles in the regulation of intracellular pH, cellular Na^+ content, and cell volume [reviewed in refs (*1*−*3*)].

Escherichia coli has two Na^+ (and Li^+)-specific Na^+/H^+ antiporters encoded by *nha*A and *nha*B (*4*−*6*). NhaA is the Na^+/H^+ antiporter that is essential for $H^+$and Na^+ homeostasis in *E. coli* (*1*, *5*).

The NhaA protein is predicted to have a putative secondary structure consisting of 12 TMS[1] connected by hydrophilic loops (*7*). This predicted topology that has been substantiated biochemically (*7*, *8*) has recently gained strong support from cryo-electron microscopy of NhaA 2D crystals (*9*). Both in the crystals as well as in the native membrane, NhaA forms oligomers (*10*).

NhaA is an electrogenic antiporter that has been purified to homogeneity and reconstituted in a functional form in proteoliposomes (*11*). The H^+/Na^+ stoichiometry of NhaA is $2H^+/Na^+$ (*12*). The activity of NhaA is highly dependent on pH, with the V_{max} changing by over 3 orders of magnitude from pH 7 to 8, suggesting that NhaA is equipped with both a "pH sensor" and a transducer to increase its activity with pH.

A series of studies showed that His-225 plays a primary role in the pH regulation of NhaA and that this is most likely accomplished by its capacity to form hydrogen bonds (*13*, *14*). Gly-338 was also found to affect the pH response of NhaA; its replacement with serine (G338S) produced a transporter which, in contrast to the wild-type protein, lacks pH control (*15*). Other residues have been implicated in the pH response of NhaA (*15*, *16*).

pH-induced conformational changes are required for the pH regulation of NhaA. The conformational changes involve loop VIII−IX (*17*) and the N-terminal loop of NhaA (*18*).

Neither NhaA nor any other secondary transporter has been solved at atomic resolution. Therefore, residues involved in the binding of the cations and/or their translocation can only be indirectly inferred. One approach is site-directed mutagenesis of residues which have the capacity to attract, bind, or repel cations. The mutagenesis is done in plasmid-encoded *nha*A, and the mutants are analyzed for their ion transport properties in bacterial host devoid of antiporter activity. The functional and structural importance of charged residues located in hydrophobic transmembrane regions has been postulated for many ion-coupled transporters (*19*−*24*). According to the model proposed for the secondary structure of NhaA, six charged residues are located in putative TMS; four Asp residues in the N terminal region (Asp-65, Asp-133, Asp-163, and Asp-164) and two Lys residues in the C terminus (Lys-300 and Lys-362). With the exception of Lys-362 which can be replaced with arginine, these residues are

† This research was supported first by a grant from the GIF, the German−Israeli Foundation for Scientific Research and Development (to E.P.), and then by the BMBF and the International Bureau of the BMBF at the DLR [German−Israeli Project Cooperation on Future Oriented Topics (DIP) (to E.P.)]. A. Rothman was partially supported by a fellowship from the Moshe Shilo Center for Biogeochemistry. E.P. was supported by the Massimo and Adelina Della Pergolla Chair in Life Sciences.

* Corresponding author. Tel: 972-2-6585094. Fax: 972-2-6586947. Email: etana@vms.huji.ac.il.

[1] Abbreviations: TMS, transmembrane segments; RSO, right-side-out membrane vesicles; ISO, inside-out membrane vesicles; ΔpH, pH gradient; PAGE, polyacrylamide gel electrophoresis; DTT, dithiothreitol; TCA, trichloroacetic acid; SH, sulfhydryl reagents; NEM, *N*-ethylmaleimide; PCMBS, *p*-chloromercuribenzenesulfonate; BTP, 1,3-bis[tris(hydroxymethyl)methylamino]propane.

10.1021/bi011655v CCC: $22.00
Published on Web 12/14/2001

conserved in all members of the family of NhaA antiporters (*1*).

In a previous study, each of the four aspartate residues in NhaA of *E. coli* has been replaced by asparagine in plasmid-encoded *nhaA*, and the constructs studied in an *E. coli* mutant defective in both *nhaA* and *nhaB* (*24*). The findings suggested that Asp-133, Asp-163, and Asp-164 are essential for the functioning of NhaA.

Random mutagenesis of plasmidic *nha*A has also been used to isolate *nha*A mutations affecting ion transport by selecting for mutants that cannot support growth at high [Na^+] (0.65 M, pH 8.0) and/or high [Li^+] (0.15 M, pH 7.5) of an antiporter-defective *E. coli* strain (*16*). In contrast to the previous results, this study showed that alanine replacement of Asp-133 retains low Li^+/H^+ antiporter activity. In both of these site-directed and random mutagenesis studies, the level of the mutated NhaA proteins in the membrane has not been determined. Therefore, an effect of the mutation on expression of the genes and/or step(s) leading to assembly of the protein in the membrane has not been excluded.

In a previous study (*25*), we therefore constructed Cys-replacement mutations of Asp-133 (D133C), Asp-163 (D163C), and Asp-164 (D164C) and confirmed that both Asp-163 and Asp-164 are essential. Their Cys-replacements were fully expressed but inactive.

However, D133C which was also expressed exhibited the most interesting characteristics, affecting dramatically the K_m of the antiporter to the ions. In the present work, we further studied this residue and its topology in the membrane using a Cys-less derivative of D133C (C-less D133C). Our results show that D133 is involved in the ion translocation by NhaA and although according to the topology model of NhaA D133 is located in the middle of TMS IV (*7*), this residue is exposed to an aqueous environment continuous with the cytoplasm. These results led us to focus on TMS IV of NhaA. The construction of a second mutation in TMS IV, T132C, was motivated by the suggestion that the hydroxyl and carboxyl in juxtaposition participate in the Na^+ binding site of a Na^+/ATPase (*26*).

Three additional mutations have previously been identified in helix IV (*15*), as suppressors of G338S, a mutant that cannot grow at alkaline pH in the presence of Na^+ because its antiporter is not regulated by pH. These included A127V, A127T, and P129L. Therefore, the latter three mutations were also further studied here. Interestingly, the mutation A127V was also obtained in the present work but with a different selection procedure—random mutagenesis of wild-type *nha*A and selection of mutants that grow on high Na^+ but not high Li^+ at neutral pH.

Kinetic analysis revealed that the mutants clustering in helix IV can be divided into two types. One type (D133C, T132C, and P129L) affects the ion transport activity of NhaA but not its dependence on pH. The other type (A127V and A127T) affects both the ion translocation as well as the pH regulation of the antiporter. Given that TMS forms a α-helix, the first type of residues are localized on one face whereas the latter are on the opposite face of the helix.

MATERIALS AND METHODS

Bacterial Strains and Culture Conditions. EP432 is an *E. coli* K-12 derivative, which is *mel*BLid, Δ*nha*A1::*kan*, Δ*nha*B1::*cat*, Δ*lac*ZY, thr1 (*6*). TA16 is *nha*A^+*nha*B^+*lacI*^{Q} (TA15*lacI*^{Q}) and otherwise isogenic to EP432 (*11*). DH5α (U. S. Biochemical Corp.) was used as a host for construction of plasmids. Cells were grown either in L broth (LB) or in modified L broth (LBK) in which NaCl was replaced by 87 mM KCl, pH 7.5. Where indicated, the medium was buffered with 60 mM BTP, and the pH was titrated with HCl. Cells were also grown in minimal medium A without sodium citrate (*27*) with 0.5% glycerol, 0.01% $MgSO_4 \cdot 7H_2O$, and thiamin (2.5 μg/mL). When required, threonine (0.1 mg/mL) was added. For plates, 1.5% agar was used. Antibiotics were 100 μg/mL ampicillin and/or 50 μg/mL kanamycin. The resistance to Li^+ and Na^+ was tested by growing EP432-transformed cells on LB plates (24 h at 37 °C) or in liquid medium containing 0.6 M NaCl (pH 8.3) or 0.2 M LiCl (pH 8.3) at 37 °C.

Plasmids. Plasmid pGM36 is a pBR322 derivative carrying wild-type *nhaA* (*28*). Plasmid pAXH (previously called pYG10) is a pET20b (Novagen) derivative carrying His-tagged *nhaA* (*8*). pC-less AXH was described previously (*8*). pC-less XH2 was derived from pC-less AXH by excision of the *Bsh*1365I−*Bsh*1365I fragment (252 bp) and ligation. This plasmid lacks *Bgl*II in position 3382. pGMAR100 is a derivative of pGM36 carrying native *nha*A (*15*). pECO is a derivative of pGMAR100 with an *Eco*RI site in position 5319. All plasmids carrying mutations are designated by the name of the plasmid followed by the mutation. pAXH-D133C, pAXH-D163, and pAXH-D164C were derived from pAXH as described previously (*25*).

*Site-Directed Mutagenesis of nha*A. The polymerase chain reaction-based protocol (*29*) was used for site-directed mutagenesis. In each case, the entire fragment originated by polymerase chain reaction (PCR) and cloned in a plasmid was sequenced through the ligation junctions to verify the accuracy of mutagenesis. This routine ensured that the entire *nha*A gene did not harbor mutations in addition to the one described.

To generate D133C in a Cys-less background, the *Bgl*II−*Bgl*II fragment (788 bp) of pAXH-D133C (*25*) was ligated with the *Bgl*II−*Bgl*II fragment (4.2 kb) of pC-less AXH. For Cys-replacement of Thr132, pGMAR100 was used as a template with the mutagenic primers described in Table 1. The resulting plasmid was pGMAR100-T132C. For construction of this mutation in pAXH (pAXH-T132C), a *Nhe*I−*Mlu*I fragment (879 bp) of the resulting PCR product was ligated to a *Nhe*I−*Mlu*I (4.1 kb) fragment of pAXH. To generate the T132C mutation in a Cys-less background, the *Bgl*II−*Mlu*I fragment of pGMAR100-C-less (682 bp) was ligated with the *Bgl*II−*Mlu*I fragment (4.6 kb) of pGMAR100-T132C, yielding pGMAR100-C-less T132C. To generate His-tagged-C-less-T132C, the *Eco*RI−*Bgl*II fragment (465 bp) of pAXH-T132C was ligated with a *Eco*RI−*Bgl*II fragment (4.3 kb) of pC-less XH2, resulting in pC-less XH2-T132C. To generate pGMAR100-A127T, an *Ava*I−*Mun*I fragment (533 bp) of the double mutant pGMAR100-A127T/G338S (*15*) was ligated to an *Ava*I−*Mun*I (4.8 kb) fragment of pGMAR100. For Cys-replacement of Ala-127, pECO was used as a template with the mutagenic primers described in Table 1. The resulting plasmid was pECO-A127C. For construction of this mutation in pAXH and in a His-tagged-C-less background, an *Eco*RI−*Bgl*II fragment (467 bp) of the resulting PCR product was ligated

Table 1: Studied Mutations in Helix IV of *nha*A[a]

mutation	DNA sequence of mutagenic oligonucleotide	codon change observed	ref
A127V[b]		GCG→GTG	this study and (*15*)
A127T[b]		GCG→ACG	this study and (*15*)
A127C	CGAAGGGTGG**TGT**ATA[a]CCGGCGGC	GCG→TGT	this study
P129L[b]		CCG→CTG	(*15*)
P129C	GAAGGGTGGGC**C**A[a]T**ATGC**GCGGCTAC	CCG→TGC	this study
T132C	CCGGCGGCA**AC**[a]**T**GACATTGCTTTTGC	ACT→TGC	this study
D133C	CGGCTACT**TG**CATTGCTTTTGCACTTGGTGTACTGGC	GAC→TGC	(*25*)
end primers for mutations	sense primer TTTAACGATGATTCGTGGCGG		
	antisense primer GCTCATTTCTCTCCCTGATAAC	none	

[a] The mutated bases are shown in boldface type. Additional substitutions have been introduced to create silent mutations in Thr-132, Pro-129, and Ala-127 that generate the unique restriction sites *Sph*I, *Nde*I, and *Acc*I, respectively, in the DNA sequence of *nha*A. [b] Mutations obtained by random mutagenesis.

to an *Eco*RI−*Bgl*II (4.9 kb) fragment of pAXH and pC-less XH2, respectively. pGMAR100-A129L was constructed as described in ref *15*.

For Cys-replacement of Pro129, pGMAR100 was used as a template with the mutagenic primers described in Table 1. The resulting plasmid was pGMAR100-P129C. To generate P129C mutation in a Cys-less background, the *Bgl*II−*Mlu*I fragment (4.6 kb) of pGMAR100-P129C was ligated with the *Bgl*II−*Mlu*I fragment (682 bp) of pGMAR100-C-less, yielding pGMAR100-C-less P129C. To generate His-tagged-P129C, the *Nhe*I−*Mlu*I fragment (879 bp) of pGMAR100-C-less P129C was ligated with a *Nhe*I−*Mlu*I fragment (4.1 kb) of pAXH, resulting in pAXH-P129C. To generate His-tagged-C-less-P129C, the *Eco*RI−*Bgl*II fragment (465 bp) of pAXH P129C was ligated with a *Eco*RI−*Bgl*II fragment (4.3 kb) of pC-less XH2, resulting in pC-less XH2-P129C.

Random Mutagenesis and Selection of A127V. Random mutagenesis was conducted in vitro by hydroxylamine/hydrochloride on plasmid pGMAR100 encoding wild-type *nha*A as described (*15*). The mutated plasmid was transformed into a strain (EP432) lacking both antiporter genes *nha*A and *nha*B and selection of *nha*A mutants that grow on high [Na^+] (0.6 M in LBK medium) but not high [Li^+] (0.1 M in minimal medium) at neutral pH. This selection was possible since EP432 does not grow under these selection conditions unless transformed with functional plasmid-encoded *nha*A (*6*). Two identical mutations were found independently and identified as A127V.

Preparation of Inside-Out (ISO) Membrane Vesicles, Assay of Na^+/H^+ and Li^+/H^+ Antiporter Activities, and Quantitation of NhaA in the Membranes. EP432 cells transformed with mutant or wild-type *nha*A-expressing plasmids were grown, and everted vesicles were prepared and used to determine the Na^+/H^+ or Li^+/H^+ antiporter activity as described (*30*, *31*). A fluorescence assay of antiport activity was performed as described (*31*) using acridine orange to measure generation of ΔpH. After energization with Tris−D-lactate or ATP as indicated, quenching of the fluorescence was allowed to achieve a steady state, and then either Na^+ or Li^+ was added. A reversal quenching (dequenching) indicates that H^+ is exiting the vesicle in antiport with the indicated cation. NhaA either in everted membrane vesicles or in purified form was quantitated by Western analysis using an anti-NhaA monoclonal antibody [mAb 1F6, (*32*)] as described previously (*13*). Total membrane protein was determined according to (*33*).

Purification of His-Tagged Antiporters. TA16 cells were transformed with wild-type or mutant *nha*A-expressing plasmids (pAXH derivatives). *nha*A induction and membrane preparation were carried out as described in ref *11*, except that the resuspension buffer did not contain DTT. Membrane solubilization and affinity purification of the His-tagged antiporters were as described (*8*). If not otherwise indicated, the eluted protein (200 μL) was precipitated in 10% TCA for 30 min at 4 °C, collected by centrifugation (14000*g*, 30 min), resuspended in sample buffer, and resolved on a 12.5% SDS−PAGE prepared according to (*34*).

Determination of Accessibility to NEM and PCMBS. TA16 cells were transformed with wild-type or mutant *nha*A-expressing plasmid. Preparation of ISO membrane vesicles was carried out as described above with no DTT in the resuspension medium. RSO membrane vesicles were prepared by lysozyme ethylenediaminetetraacetic acid treatment and osmotic lysis as described (*35*). RSO or ISO membrane vesicles (200 μg) were resuspended in 500 μL containing 100 mM KP_i, pH 7.5, and 5 mM $MgSO_4$. *p*-Chloromercuribenzenesulfonate (PCMBS) (0.2 mM) was added, and the membranes were incubated for different time periods as indicated, at room temperature. Membranes were washed 4 times in 3 mL of solution, and treated with [^{14}C]NEM for assaying NEM-titratable residues using 0.5 mM [^{14}C]NEM (specific activity of 4 μCi/μmol) as described (*8*). Where indicated, intact cells were used instead of RSO membrane vesicles for treatment with PCMBS (10 mM), and then the NEM-titratable residues were quantitated in membrane vesicles isolated by sonication as described (*8*). Treatment with nonradioactive NEM was as described (*8*).

RESULTS

Construction of Mutations in Helix IV. By combining site-directed and random mutagenesis, kinetic studies, and Cys-accessibility analysis, we show that putative TMS IV of the NhaA-Na^+/H^+ antiporter (Figure 1) is involved both in ion translocation as well as in pH regulation of the antiporter.

All plasmid-encoded mutants of TMS IV studied in this work, D133C, T132C, P129L, A127V, and A127T (Table 1), were also constructed and studied in a Cys-less background. When indicated, the mutation was replaced with Cys. It should be noted that due to an error in the DNA sequencing, A127T was previously considered to be A130T (*15*).

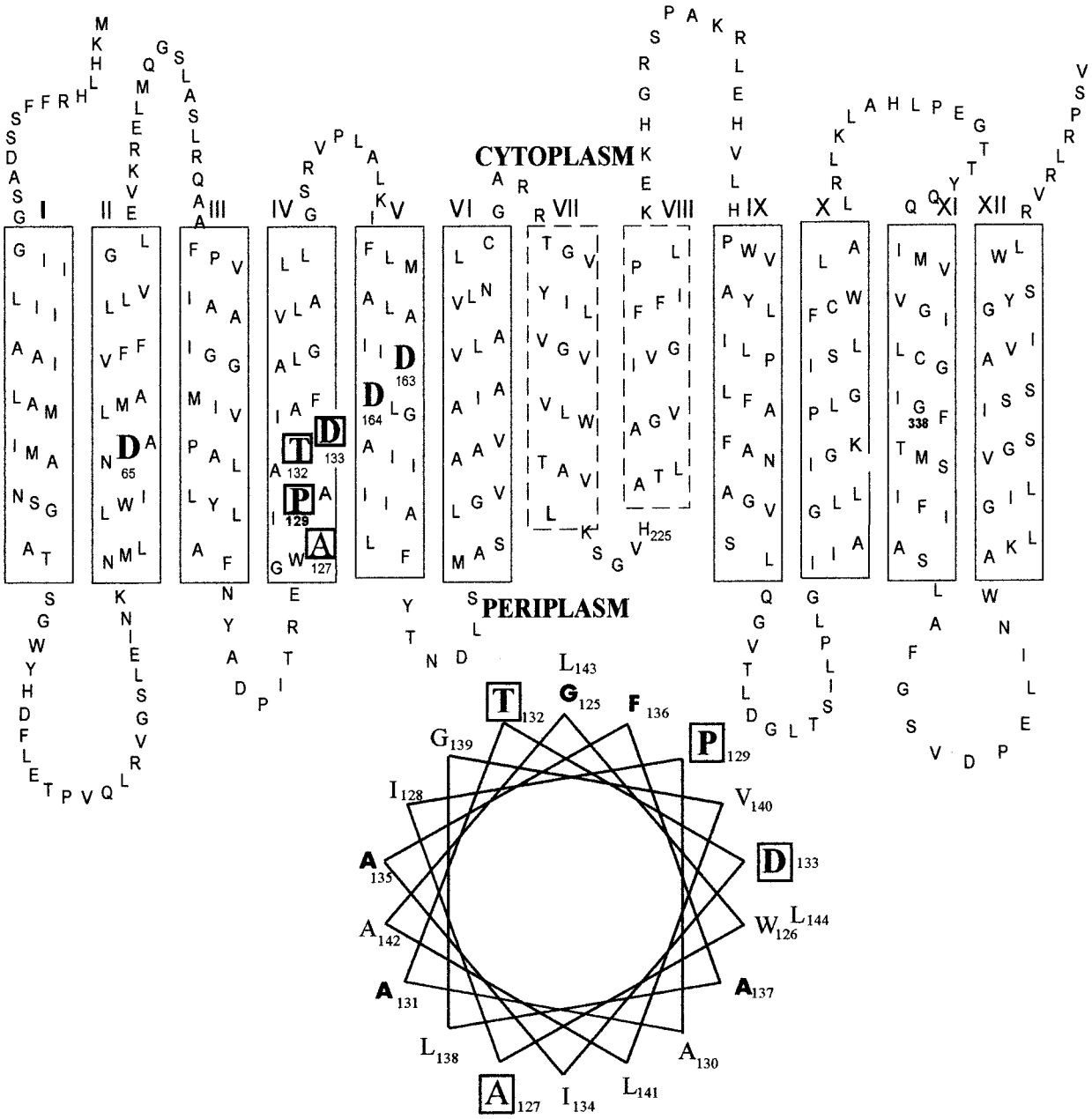

FIGURE 1: Secondary structure model of NhaA. The 12 transmembrane segment model proposed for the topology of NhaA is shown (*7*). The single-letter amino acid code is used, and the location in the amino acid sequence is indicated by a number. The Roman numerals indicate the numbers of the TMS. Residues mutated in this work are shown enclosed in squares. Residues located in putative α-helices that were mutated and shown to affect the antiporter activity [(*16*, *24*, *25*) and this work] are enlarged. Residues that are conserved (*3*) are shown in boldface type. Helical-wheel presentation of TMS IV is also shown at the bottom.

The plasmid-encoded *nha*A mutants were transformed into EP432 for growth phenotype analysis. All mutants were capable of growth in high [Na^+], both at neutral pH (data not shown) as well as at alkaline pH (Table 2). All mutants except for A127V grew in the presence of Li^+ at pH 7 (data not shown) and at pH 8.3 (Table 2). While the expression of C-less D133C was 10% of that of the wild-type, the expression of all other mutants was very similar to that of the wild-type as determined by Western analysis with a monoclonal antibody (*32*) directed against the N-terminus of the protein (Table 2). It should be noted that since all mutations are expressed from multicopy plasmids, the lowest level of expression observed here is much higher than that observed from a single-copy chromosomal *nha*A which even cannot be detected by the Western analysis (*13*).

Mutations in Asp-133, Thr-132, Ala-127, and Pro-129 Affect the Apparent K_m of NhaA. Inside-out membrane vesicles were prepared from nontransformed EP432 cells (negative control) or from EP432 cells transformed with wild-type (positive control) or mutant *nha*A-expressing plasmids, and the Na^+/H^+ and Li^+/H^+ antiporter activities were measured at pH 8.5 as recovery from the respiration-dependent fluorescence quenching of acridine orange upon addition of either Na^+ or Li^+ (Figure 2 and Table 2).

Membranes derived from EP432 cells transformed with the vector plasmid have no Na^+/H^+ or Li^+/H^+ antiporter activity (*6*). Transformation with the wild-type *nha*A plasmid restores both Na^+/H^+ and Li^+/H^+ antiporter activities [(*6*), Figure 2 and Table 2]. At pH 8.5, although reduced to certain levels, all mutants except for A127V showed significant Na^+/

Table 2: Phenotype of NhaA Mutants[a]

	expression levels in EP432 (%)	growth		antiporter activity (%)	
		Na^+	Li^+	Na^+	Li^+
wild-type	100	+	+	100	100
A127V	98	+	−	7	67
A127T	96	+	+	41	100
A127C	90	+	+	100	100
C-less A127C	92	+	+	90	90
P129L	100	+	+	38	81
P129C	100	+	+	100	100
C-less P129C	99	+	+	100	100
T132C	95	+	+	54	91
C-less T132C	95	+	+	63	87
D133C	98	+	+	87	70
C-less D133C	10	+	+	63	72

[a] EP432 transformed with plasmid expressing the wild-type or the indicated mutations was used to produce everted membrane vesicles. Quantitation of NhaA in everted membrane vesicles was conducted by Western analysis using a monoclonal antibody (1F6) against the N-terminus of NhaA (*32*) and expressed in % [100% = the level in the wild-type (wt)]. Growth on high Na^+ or high Li^+ was determined on LB plates containing either 0.6 M NaCl at pH 8.3 or 0.2 M LiCl at pH 8.3: (+) growth; (−) no growth. Antiporter activity was measured at pH 8.5 as described in Figure 2 and expressed in % (100% = percent of dequenching observed in wild-type membranes). Where indicated, either Na^+ or Li^+ (10 mM each) was used to elicit dequenching.

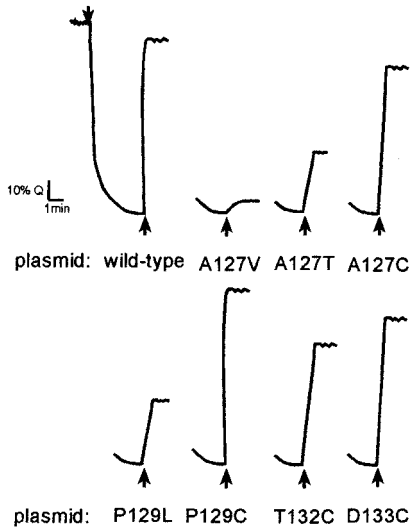

FIGURE 2: Na^+/H^+ antiporter activity in everted membrane vesicles of the NhaA mutants. Cells were grown in LBK (pH 7.5), and membrane vesicles were prepared from Δ*nha*AΔ*nha*B *E. coli* strain (EP432) transformed with control plasmid bearing wild-type *nha*A or derivatives carrying the indicated various mutations in *nha*A as specified in Table 2. ΔpH was monitored in everted membrane vesicles (50 μg of protein) with acridine orange (0.5 μM) at pH 8.5 as described under Materials and Methods. At the onset of the experiment, Tris−D-lactate (5 mM) was added (arrow pointing down), and the fluorescence quenching (*Q*) was recorded. NaCl (10 mM, arrows pointing up) was then added, and the new steady state of fluorescence obtained (dequenching) after each addition was monitored. All experiments were repeated at least 3 times, and the results were essentially identical.

H^+ and Li^+/H^+ antiporter activity, varying between 40% and 100% of the wild-type activity (Figure 2 and Table 2). At this pH, the Li^+/H^+ antiporter activity of A127V was 67%, but its Na^+/H^+ activity was only 7% of that of the wild-type (Figure 2 and Table 2). The apparent K_m and V_{max} of all these mutants were determined for both ions at pH 8.5 and compared with the values of the wild-type NhaA (Table 3). Apart from A127V with a V_{max} for Na^+ of only 10%, the other mutants showed a V_{max} for both ions between 40% and 100% of that of the wild-type NhaA. Whereas the Cys-replacements A127C and P129C showed K_m values for both ions similar to that of the wild-type, the mutants A127V, A127T, P129L, T132C, and D133C showed a dramatic change in the apparent K_m for both ions. For example, the K_m of D133C-NhaA for Na^+ and Li^+ was 18- and 62-fold higher, respectively, than that of the wild-type NhaA (Table 3). The other mutants showed even higher differences as compared to the wild-type NhaA (Table 3).

Table 3: Mutations Affecting the Apparent K_m of NhaA[a]

mutation	K_m (mM) (for Na^+)	K_m (mM) (for Li^+)	V_{max} (%) (for Na^+)	V_{max} (%) (for Li^+)
wild-type	0.2	0.02	100	100
A127V	13.2	5.4	10	79
A127T	12.6	0.62	41	100
P129L	5.6	0.79	38	87
T132C	12.4	0.7	90	95
D133C	3.6	1.24	91	84
A127C	0.24	0.02	100	100
P129C	0.4	0.028	100	100

[a] EP432 was transformed with wild-type or mutant *nhaA*-expressing plasmids. The Na^+/H^+ or Li^+/H^+ antiporter activities of NhaA were measured in everted membrane vesicles prepared from EP432, in the presence of different concentrations of NaCl (0.1−100 mM) or LiCl (0.1−100 mM) at pH 8.5. The K_m and V_{max} values were calculated by linear regression of a Lineweaver−Burk plot.

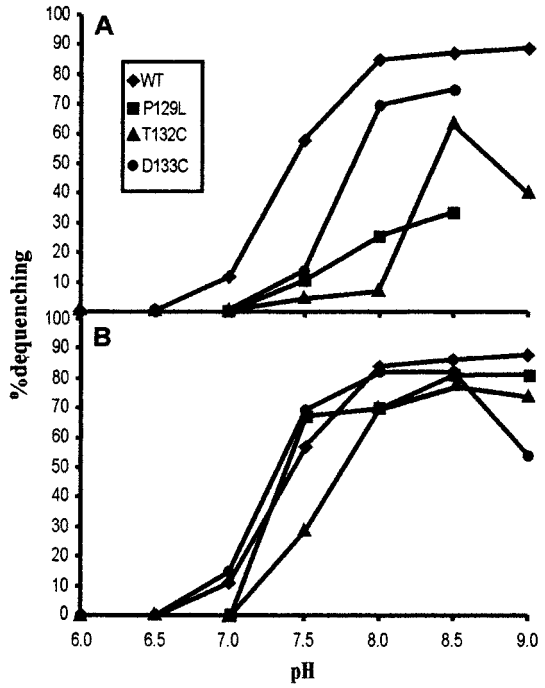

FIGURE 3: Effect of pH on NhaA mutations (P129L, T132C, and D133C) that affect the K_m of ion translocation. Preparation of inverted membrane vesicles and measurement of the Na^+-dependent change in ΔpH were as described in Figure 2. The activity of wild-type NhaA (◆) and the indicated mutants was measured at the indicated pH values at Na^+ concentrations of 10 mM (A) and 100 mM (B). WT, wild-type NhaA. All experiments were repeated at least 3 times, and the results were essentially identical.

Effect of pH on the NhaA Mutations. Since NhaA is dramatically dependent on pH (*11*, *13*), it was interesting to test the pH dependence of the mutations that affect the apparent K_m of NhaA to the ions (Figures 3A and 4A). It is apparent that compared to the wild-type antiporter the pH

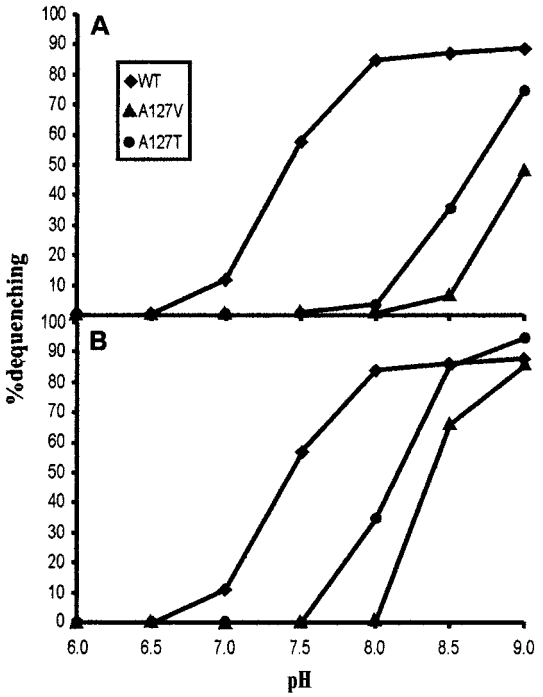

FIGURE 4: Effect of pH on NhaA mutations, A127V and A127T. The experimental procedure was as in Figure 3. WT, wild-type NhaA. For comparison, the pH profile of the wild-type NhaA is reproduced from Figure 3.

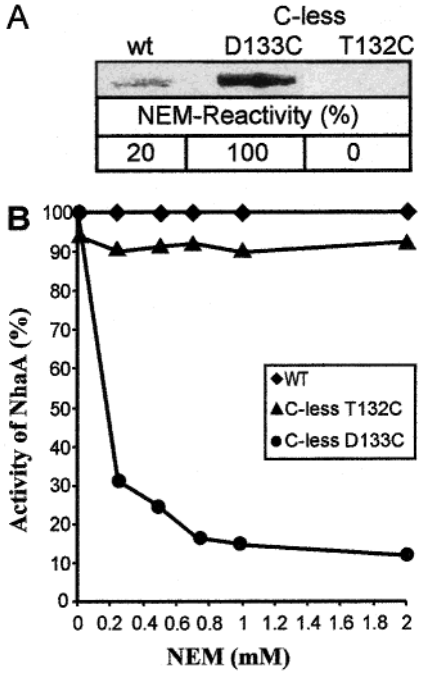

FIGURE 5: Alkylation of C-less-T132C, C-less-D133C, and wild-type NhaA by [^{14}C]NEM and effect of NEM on the Na^+/H^+ antiporter activity. (A) Membrane vesicles (200 μg of total protein) derived from TA16 cells expressing wild-type NhaA from plasmid pAXH, C-less-T132C, or C-less-D133C (the former constructed in pC-less AXH2, the latter in pC-less AXH). The mutants in C-less NhaA were incubated with [^{14}C]NEM as described under Materials and Methods. The membranes were washed, solubilized, and affinity-purified. The purified protein samples were acid-precipitated as described under Materials and Methods, and equal volumes were resolved on a 12.5% SDS−PAGE prepared as described (*34*). The dry gel was exposed to a Phospho-imager (Fuji Bas 1000), and the radioactive bands were quantitated. The autoradiogram and its quantitation are shown. The intensities are expressed in % (100% = the maximal intensity observed) and have been normalized by the amount of protein as described (*8*). (B) Everted membrane vesicles prepared from EP432 cells transformed with wild-type (◆), C-less D133C (●), or C-less T132C (▲) NhaA-expressing plasmids were preincubated in the absence (controls) or presence of NEM (0.2−2 mM) for 20 min at room temperature. The membranes were washed and assayed for Na^+/H^+ antiporter activity as described under Materials and Methods. The activities were measured by the percentage of recovery from the ATP-dependent fluorescence quenching of acridine orange after addition of NaCl (10−40 mM) to the assay medium at pH 8.5 expressed as % (100% = percent of dequenching observed in wild-type membranes). WT, wild-type NhaA.

profile (at 10 mM NaCl) of the antiporter activity of each of the mutants was shifted to the basic pH range (Figures 3A and 4A). The smaller shift was observed with D133C (0.5 pH unit) and the largest with A127V and A127T (3 and 2 pH units, respectively).

We have previously shown (*11*, *13*) that the pH shift between pH 7 and 8.5 affects primarily the V_{max} of wild-type NhaA (≥1000-fold) and much less the apparent K_m (≤10-fold). We therefore compared the pH dependence of all NhaA mutants at 100 mM Na^+, a concentration supposed to saturate or approach saturation of the antiporter (Figures 3B and 4B), to the pH profile obtained at 10 mM Na^+ (Figures 3A and 4A). The results show that when the pH dependence was tested at 100 mM, the difference in the pH profiles between D133C, P129L and the wild-type NhaA completely vanished and with respect to T132C only a slight basic shift in the pH profile remained (Figure 3B). Hence, D133C, T132C, and P129L mutations affect a step(s) that is (are) reflected in the apparent K_m of NhaA but not a step crucial for the pH-regulated rate of NhaA.

The effect of pH on the kinetic parameters of A127V and A127T was remarkably different. Increasing Na^+ concentration had no effect on the pH profile. Thus, at 100 mM Na^+ as at 10 mM, the antiporter activity of A127V was shut off up to pH 8 and that of A127T up to pH 7.5 (Figure 4). Above this pH, greater activities were observed at the higher Na^+ concentrations as expected from a drastic K_m change. We suggest that these mutations affect both the pH profile and the K_m of NhaA.

Accessibility to NEM and Its Effect on Na^+/H^+ Antiporter Activity. NEM is a SH membrane-permeant reagent that reacts with Cys residues in membrane proteins given they are exposed to aqueous environment allowing ionization. We therefore tested the accessibility to NEM of the Cys-replacement mutants of NhaA. To avoid complexity due to the native cysteine of NhaA, we constructed for these experiments the Cys-replacement mutations in His-tagged-Cys-less-NhaA of which all native cysteines were replaced with serines (*8*). The growth phenotypes of the mutants constructed in the Cys-less background were similar to those constructed in the wild-type (Table 2 and data not shown).

Everted membrane vesicles isolated from TA16 cells expressing mutant or wild-type His-tagged NhaA derivatives were incubated with [^{14}C]NEM. The His-tagged antiporters were then affinity-purified, and the radioactivity of the purified protein was measured (Figure 5A and Figure 6, control lanes in A and B).

As described previously (*8*), the alkylation assay showed that the native cysteines of NhaA are hardly alkylated by NEM (Figure 5A). Similarly, very weak or no alkylation was

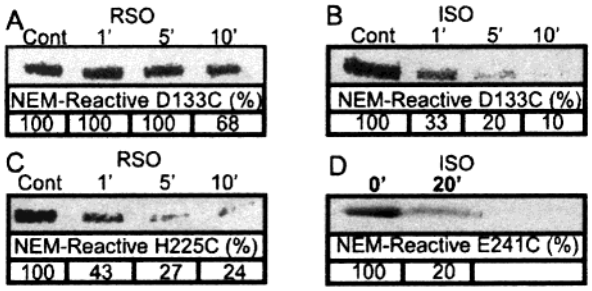

FIGURE 6: Exposure of D133C, H225C, and E241C to PCMBS in RSO or ISO membrane vesicles. (A and B) RSO (A) or ISO (B) membrane vesicles (200 μg of total protein) isolated from cells (TA16/pC-less-AXH D133C) expressing His-tagged D133C NhaA were resuspended in 500 μL containing 100 mM KPi (pH 7.5) and 5 mM $MgSO_4$. PCMBS (0.2 mM) was added, and the membranes were incubated for 1, 5, or 10 min at room temperature. As a control (Cont), membranes were incubated in the absence of PCMBS for 10 min at room temperature. Membranes were washed, treated with [^{14}C]NEM, solubilized, and affinity-purified as described under Materials and Methods. The purified protein samples were precipitated as described under Materials and Methods, and equal volumes were resolved on a 12.5% SDS−PAGE prepared as described (*34*). The dry gel was exposed to a Phospho-imager Fuji Bas 1000, and the radioactive bands were quantitated. The autoradiogram and the quantitated results are shown. The intensities are expressed in % (100% = the intensity observed in the controls) and have been normalized by the amount of protein as described under Materials and Methods. (C) RSO membrane vesicles isolated from TA16/pC-less-AXH-H225C cells were treated as in (A). (D) ISO membrane vesicles isolated from TA16/pC-less-AXH-E241C cells were treated as in (B). The autoradiograms and their quantitation are shown. The intensities are expressed in % (100% = the intensity observed in the control) and have been normalized by the amount of protein as described under Materials and Methods.

obtained with T132C (Figure 5A), A127C, and P129C whether the Cys-replacements were constructed in His-tagged wild-type or Cys-less-NhaA background (data not shown). In contrast, in both background genotypes of NhaA, D133C (Figures 5A, 6A,B) was strongly alkylated by [^{14}C]NEM.

In parallel, we tested the effect of NEM on the Na^+/H^+ antiporter activity. For this purpose, everted membrane vesicles prepared from EP432 cells transformed with plasmids expressing the NhaA variants or wild-type NhaA were incubated with NEM, washed, and assayed for Na^+/H^+ antiporter activity. The Na^+/H^+ antiporter activities of T132C (Figure 5B), A127C, and P129C (data not shown) and the wild-type NhaA (Figure 5B) were not affected by treatment of the membranes with NEM (up to 2 mM). These results are consistent with the low degree of alkylation of these Cys-replacement mutants and native cysteinyl residues of the wild-type NhaA by NEM.

In contrast, D133C NhaA (data not shown) as well as C-less-D133C (Figure 5B) were strongly affected by NEM. Treatment of membranes with 1 mM NEM inhibited up to 94% of the Na^+/H^+ antiporter activity of the mutant (Figure 5B).

The presence of Na^+ in the alkylation medium (up to 100 mM) did not affect the degree of labeling of D133C NhaA by NEM or reduce significantly the inhibitory effect of NEM on the antiporter activity of this mutant (data not shown). Therefore, we cannot ascertain that NEM and Na^+ compete for a similar binding site in D133C NhaA.

Membrane Topology of D133C. The membrane topology of D133C, the NEM-accessible residue, was studied by probing the accessibility to a membrane-impermeant SH reagent (PCMBS), both in ISO and in RSO membrane vesicles. Accessibility to PCMBS in RSO or ISO membranes implies that this residue is located or exposed at or near the face of the membrane exposed to the side of application of the reagent. Inaccessibility to PCMBS in RSO and ISO membrane vesicles implies that this residue is located in transmembrane regions. Previous studies have shown that His-225 is located and exposed at the periplasmic domain of the membrane (*8*) whereas E241 is exposed to the cytoplasm (*36*). Therefore, the accessibility of these residues to PCMBS in RSO and ISO membrane vesicles respectively served as controls in this study. For these experiments, ISO or RSO membrane vesicles were prepared from TA16 cells expressing His-tagged derivatives of C-less D133C, H225C, or E241C. The membrane vesicles or cells were first exposed to PCMBS and washed, and then exposed to [^{14}C]NEM, washed, and solubilized, and the His-tagged antiporters were affinity-purified. The level of alkylation by NEM was determined by radioactive quantitation of the His-tagged proteins separated on SDS−PAGE. The reactivity to PCMBS was determined by the difference in the number of NEM-alkylatable residues before and after exposure to PCMBS.

Treatment with PCMBS for up to 10 min did not reduce significantly the number of NEM-titratable D133C residues in RSO membrane vesicles (Figure 6A). In contrast, treatment with PCMBS reduced the number of NEM-titratable D133C residues in ISO membranes to 33% after only 1 min and to 10% after 10 min (Figure 6B). These results are similar to those obtained with E241C, a residue that is known to be exposed at the cytoplasmic face of the membrane [(*36*) and Figure 6D]. H225C, a residue which is known to be exposed to the periplasm, gave opposite results, i.e., reactive with PCMBS only in RSO membrane vesicles [(*8*) compare Figure 6A and Figure 6C]. Taken together, these results indicate that D133C is much more reactive to PCMBS in ISO than in RSO membrane vesicles, and suggest that this residue is exposed at the cytoplasmic face of the membrane.

According to the proposed model for the secondary structure of NhaA (*7*), Asp-133 is located in the middle of putative TMS IV (Figure 1). However, the results described in the present study suggest that this residue is not surrounded by a hydrophobic environment, but is rather exposed to an aqueous medium continuous with the cytoplasm.

DISCUSSION

We have previously shown that the activity of NhaA is regulated by pH and found residues (*13*−*15*) and domains involved in conformational changes (*17*, *18*, *37*) that participate in the pH regulation. Thus, mutations H225R (*13*) and G338S (*15*) were found to dramatically affect the pH dependence of the rate but not the K_m (to Na^+ or Li^+) of NhaA. In the present work, two novel types of NhaA mutations were identified: one type (D133C, T132C, and P129L) affects the apparent K_m of NhaA to the cations with no significant effect on the pH dependence of the rate of the antiporter activity. These mutations do not shift the pH profile when measured at saturating Na^+ concentration (Figure 3B) or Li^+ concentration (data not shown). In contrast, the other type of mutations (A127V and A127T) was found to affect both the K_m and the pH dependence of

the rate of NhaA activity. Accordingly, at saturating Na^+ concentration (Figure 4B) or Li^+ concentration (data not shown), the mutational change in the pH profile was maintained in these mutants. These results imply that residues involved in the ion translocation of NhaA may (A127) or may not (D133, T132, P129) overlap with those affecting the pH response of NhaA. An effect on the pH response can be due to a change in the K_m for H^+ and/or a change in a pH regulatory site, ca. a "pH sensor". At present, we cannot differentiate between these alternatives.

Interestingly, the two types of mutations have previously been isolated as suppressor mutations of NhaA-G338S, a mutant that lost pH control and therefore the capacity to shut off the antiporter and to support growth of EP432 at alkaline pH in the presence of Na^+ (*15*). Our results here confirm that the capacity to down-regulate the antiporter is the basis of this suppression. They also show two mechanisms by which this suppression can be obtained: a drastic increase in K_m in the case of P129L, but both an increase in the K_m as well as an alkaline shift in the pH profile in the case of A127V and A127T. Furthermore, our work shows that there are at least two independent selection procedures to obtain mutation A127V. Here, A127V was obtained by a procedure aimed at isolating NhaA mutants with modified K_m; growth of EP432 transformed with randomly mutated plasmidic wild-type NhaA, in the presence of Na^+ but not of Li^+, at neutral pH. Previously A127V was obtained by selecting for suppressor mutations of plasmid-encoded G338S, restoring growth of EP432 at alkaline pH in the presence of Na^+ (*15*).

Why do the mutants that affect dramatically the K_m of the antiporter to Na^+ and Li^+ still confer a growth phenotype with respect to the ions (except A127V) similar to that of the wild-type phenotype (Table 2)? The increased K_m values for Na^+ of the mutants are between 3.6 and 13.2 mM (Table 3). Therefore, the mutated NhaAs still maintain $[Na^+]_{in}$ around 10 mM. We have previously found that up to intracellular concentrations of 10−15 mM at pH 7.5 the cells grow normally (*38*). It is also puzzling why the plasmidic mutant A127V supports growth of EP432 at pH 8.3 on Na^+ (Table 2) while everted membrane vesicles derived from it do not show Na^+/H^+ activity at this pH (Figure 4). It is possible that NhaA-A127V is unstable or inactive in the membrane while it is active in vivo. The first alternative is unlikely since the mutant is expressed from a multicopy plasmid and its level of expression is 98% of that of the wild-type NhaA expressed from an isogenic plasmid (Table 2). The second alternative is also unlikely since at pH 8.5 the A127V antiporter is active and reaches 100% activity in the presence of saturating Na^+ concentration (Figure 4). We therefore suggest that a very low activity which is not detected by the assay exists and is enough to support growth of EP432 in the presence of Na^+. With regard to Li^+ , the mutated K_m values of all mutants except A127V are much lower than that for Na^+ (Table 3). Therefore, although Li^+ is much more toxic than Na^+ (*38*) and the toxic intracellular concentration of Li^+ is still not known, we can speculate that these mutated antiporters can still reduce intracellular Li^+ to below the toxic concentration (Table 2). The largest increase in K_m of A127V (Table 3) can account for its highest sensitivity to Li^+.

Our results show that amino acid residues D133, T132, A127, and P129 are not essential for the activity of NhaA. Similar results were found previously for D133 (*16*, but see ref *24*). We also showed here that Cys-replacement of A127V and P129L restores the wild-type activity of the antiporter. Nevertheless, we suggest that D133, T132, A127, and P129 and therefore helix IV, where they all cluster in the N-terminal half, are very important for the ion transport of NhaA. Accordingly, D133, T132, and P129 are evolutionary conserved residues, and A127 was replaced in evolution only with glycine [Figure 1 and (*3*)]. They affect dramatically the apparent K_m for both Na^+ and Li^+; D133C as well as C-less D133C are inactivated by NEM and are exposed to the cytoplasm despite their location in the middle of TMS IV. Remarkably, when helix IV is drawn as a helical wheel, the residues affecting the K_m, T132, D133, and P129, are located on one face of the helix (Figure 1). The other side of the helix contains A127, the residue that affects both the K_m as well as the pH regulation of NhaA.

The importance of charged residues in transmembrane domains has been well documented in many membrane transporters. One important role is the pairing with an opposite charge to form charge pairs, within and between helixes. These are crucial for helix packing and maintenance of the native structure of the protein (*19*, *21*, *22*). Our previous results suggested that none of the charged residues in the TMS of NhaA participate in charge pairs (*25*). The other important role of charged residues is in ion binding; negative residues were implied in binding of cations (*23*) while positive residues in binding of anions (*39*, *40*). D133C may belong to the former category.

Replacement of Thr-132 increased drastically the K_m of the antiporter both to Na^+ and to Li^+. It is therefore possible that similar to the case found in the Na^+/ATPase of *P. modestum* (*26*), the couple Asp-Thr is important for binding of Na^+ and Li^+. In many Na^+-coupled transporters, hydroxylic amino acids have been implicated to play a primary role in ion translocation; two serine residues are crucial for the GLT-1 glutamate transporter (*41*); several hydroxyl-containing amino acid residues (two Ser and two Thr) are important for the sodium/iodide symporter (*42*). Serines were found important in the Na^+-coupled oxaloacetate decarboxylase of anaerobic bacteria (*43*) and the proline transporter of *E. coli* (*44*). Interestingly, mutagenesis analysis of the H^+/ATPase of *E. coli* led Zhang and Fillingham (*45*) to suggest that the X-Glu-Ser-Y or X-Glu-Thr-Y sequence may constitute a structural motif for monovalent cation binding.

The apparent affinity constant characterizing the interaction of a transporter with its substrate is a combination of the equilibrium constants of ion binding and of the kinetic constants of ion translocation. Therefore, the residues found in this work to affect the apparent K_m of the antiporter can be involved in various ways in the activity of the transporter. They can modify the binding site of the ions, a highly geometrically constrained region of the antiporter in which an optimal conformation is required for the coordination of the ions. A mutation in this region could disrupt this geometry coordination and result in decreased affinity. Cys-replacement mutation D133C changed dramatically the K_m for Na^+ and Li^+ and in addition rendered this site sensitive to SH reagents. Thus, NEM alkylated D133C and completely inhibited the transport activity. If D133C is within the ion binding site, it was expected that Na^+ would protect against both chemical modification as well as inactivation by NEM.

However, neither prediction was realized. Alternatively, therefore it might be possible that the observed mutations do not modify the sodium binding directly, but rather affect the kinetics of the conformational changes responsible for translocation. This would result in a modified K_m value with no protection by Na^+. It should be emphasized though that the mutation can be near the binding site or remote from it. In the absence of atomic resolution, none of these suggestions can be proven; we cannot rule out the possibility that all these effects of both replaceable and nonreplaceable residues occur by a conformational change at a site far remote from the cationic binding site.

REFERENCES

1. Padan, E., and Schuldiner, S. (1996) in *Handbook of Biological Physics* (Konings, W. N., Kaback, H. R., and Lolkema, J. S., Eds.) pp 501−531, Elsevier Science, Dordrecht, The Netherlands.
2. Padan, E., and Krulwich, T. (2000) in *Bacterial Stress Responses* (Storz, G., and Hengge-Aronis, R., Eds.) pp 117−130, ASM Press, Washington, DC.
3. Padan, E., Venturi, M., Gerchman, Y., and Dover, N. (2000) *Biochim. Biophys. Acta 1505*, 144−157.
4. Schuldiner, S., and Padan, E. (1996) in *Structure, Function and Molecular Biology of Na/H Exchangers* (Fliegel, L., Ed.) pp 227−249, R. G. Landes Co. Biomedical Publishers, Austin, TX.
5. Padan, E., Maisler, N., Taglicht, D., Karpel, R., and Schuldiner, S. (1989) *J. Biol. Chem. 264*, 20297−20302.
6. Pinner, E., Kotler, Y., Padan, E., and Schuldiner, S. (1993) *J. Biol. Chem. 268*, 1729−1734.
7. Rothman, A., Padan, E., and Schuldiner, S. (1996) *J. Biol. Chem. 271*, 32288−32292.
8. Olami, Y., Rimon, A., Gerchman, Y., Rothman, A., and Padan, E. (1997) *J. Biol. Chem. 272*, 1761−1768.
9. Williams, K. A., Kaufer, U. G., Padan, E., Schuldiner, S., and Kühlbrandt, W. (1999) *EMBO J. 18*, 3558−3563.
10. Gerchman, Y., Rimon, A., Venturi, M., and Padan, E. (2001) *Biochemistry 40*, 3403−3412.
11. Taglicht, D., Padan, E., and Schuldiner, S. (1991) *J. Biol. Chem. 266*, 11289−11294.
12. Taglicht, D., Padan, E., and Schuldiner, S. (1993) *J. Biol. Chem. 268*, 5382−5387.
13. Gerchman, Y., Olami, Y., Rimon, A., Taglicht, D., Schuldiner, S., and Padan, E. (1993) *Proc. Natl. Acad. Sci. U.S.A. 90*, 1212−1216.
14. Rimon, A., Gerchman, Y., Olami, Y., Schuldiner, S., and Padan, E. (1995) *J. Biol. Chem. 270*, 26813−26817.
15. Rimon, A., Gerchman, Y., Kariv, Z., and Padan, E. (1998) *J. Biol. Chem. 273*, 26470−26476.
16. Noumi, T., Inoue, H., Sakurai, T., Tsuchiya, T., and Kanazawa, H. (1997) *J. Biochem. 121*, 661−670.
17. Gerchman, Y., Rimon, A., and Padan, E. (1999) *J. Biol. Chem. 274*, 24617−24624.
18. Venturi, M., Rimon, A., Gerchman, Y., Hunte, C., Padan, E., and Michel, E. (2000) *J. Biol. Chem. 275*, 4734−4742.
19. Lee, J. I., Hwang, P. P., and Wilson, T. H. (1993) *J. Biol. Chem. 268*, 20007−20015.
20. Nakamura, T., Komano, Y., and Unemoto, T. (1995) *Biochim. Biophys. Acta 1230*, 170−176.
21. Dunten, R. L., Sahin, T. M., and Kaback, H. R. (1993) *Biochemistry 32*, 3139−3145.
22. Sahin-Toth, M., and Kaback, H. R. (1993) *Biochemistry 32*, 10027−10035.
23. Yerushalmi, H., and Schuldiner, S. (2000) *Biochemistry 39*, 14711−14719.
24. Inoue, H., Noumi, T., Tsuchiya, T., and Kanazawa, H. (1995) *FEBS Lett. 363*, 264−268.
25. Rothman, A. Ph.D. Thesis, Hebrew University of Jerusalem, Israel, 1997.
26. Kaim, G., Wehrle, F., Gerike, U., and Dimroth, P. (1997) *Biochemistry 30*, 9185−9194.
27. Davies, B. D., and Mingioli, E. S. (1950) *J. Bacteriol. 60*, 17−28.
28. Karpel, R., Olami, Y., Taglicht, D., Schuldiner, S., and Padan, E. (1988) *J. Biol. Chem. 263*, 10408−10414.
29. Ho, S. F., Hunt, H. D., Horton, R. M., Pullen, J. K., and Pease, L. R. (1989) *Gene (Amsterdam) 77*, 51−59.
30. Rosen, B. (1986) *Methods Enzymol. 125*, 328−336.
31. Goldberg, E. B., Arbel, T., Chen, J., Karpel, R., Mackie, G. A., Schuldiner, S., and Padan, E. (1987) *Proc. Natl. Acad. Sci. U.S.A. 84*, 2615−2619.
32. Padan, E., Venturi, M., Michel, H., and Hunte, C. (1998) *FEBS Lett. 441*, 53−58.
33. Bradford, W. (1976) *Anal. Biochem. 72*, 248−254.
34. Laemmli, U. (1970) *Nature 227*, 680−685.
35. Kaback, H. R., Barnes, J., and Eugene, M. (1971) *J. Biol. Chem. 246*, 5523−5531.
36. Gerchman (2000) Ph.D. Thesis, Hebrew University of Jerusalem, Israel.
37. Rothman, A., Gerchman, Y., Padan, E., and Schuldiner, S. (1997) *Biochemistry 36*, 14572−14576.
38. Harel-Bronstein, M., Dibrov, P., Olami, Y., Pinner, E., Schuldiner, S., and Padan, E. (1994) *J. Biol. Chem. 270*, 3816−3822.
39. Kolbe, M., Besir, H., Essen, L. O., and Oesterhelt, D. (2000) *Science 288*, 1390−1396.
40. Fu, D., Sarker, R. I., Abe, K., Bolton, E., and Maloney, P. C. (2001) *J. Biol. Chem. 276*, 8753−8760.
41. Zhang, Y., and Kanner, B. I. (1999) *Proc. Natl. Acad. Sci. U.S.A. 96*, 1710−1715.
42. De La Vieja, A., Dohan, O., Levy, O., and Carrasco, N. (2000) *Physiol. Rev. 80*, 1083−1105.
43. Jockel, P., Schmid, M., Steuber, J., and Dimroth, P. (2000) *Biochemistry 39*, 2307−2315.
44. Quick, M., Tebbe, S., and Jung, H. (1996) *Eur. J. Biochem. 239*, 732−736.
45. Zhang, Y., and Fillingham, R. H. (1995) *J. Biol. Chem. 270*, 87−93.

BI011655V